



## Full Length Article

## Ground state depletion – A step towards mid-IR lasing of doped silver halides

Yuval Tsur<sup>a,\*</sup>, Sharone Goldring<sup>b</sup>, Ehud Galun<sup>c</sup>, Abraham Katzir<sup>a</sup><sup>a</sup> Raymond and Beverly Sackler Faculty of Exact Sciences, Tel-Aviv University, Tel-Aviv 6997801, Israel<sup>b</sup> Applied Physics Division, Soreq NRC, Yavne 81800, Israel<sup>c</sup> DDR&D, Ministry of Defense, Israel

## ARTICLE INFO

## Article history:

Received 17 June 2015

Accepted 18 February 2016

Available online 27 February 2016

## Keywords:

Middle infrared lasers

Laser materials

Fluorescence

Absorption saturation

## ABSTRACT

We show for the first time ground state absorption saturation in a doped silver halide crystal ( $\text{AgCl}_x\text{Br}_{1-x}$ ), specifically with cobalt. Spectroscopic studies showed absorption bands in the 1.4–2.5  $\mu\text{m}$  region and emission bands in the 3.8–5.0  $\mu\text{m}$  region, with a 1.5 ms lifetime at low temperatures. Absorption saturation indicates a good low and room temperature lasing feasibility at 4.1  $\mu\text{m}$ . In addition, a comparison of cobalt, nickel and iron as dopants is presented. These doped silver halide crystals can be extruded to form optical fibers, possibly introducing a new family of fiber lasers for the middle infrared.

© 2016 Elsevier B.V. All rights reserved.

## 1. Introduction

Lasers operating in the middle infrared (mid-IR) 3–5  $\mu\text{m}$  atmospheric window have many uses, among them are trace-chemical sensing, pollution monitoring, and infrared counter-measures. Most of the coherent sources emitting in the 3–5  $\mu\text{m}$  range are currently based on either quantum cascade lasers [1] or frequency conversion devices [2]. Developing impurity doped glass or crystalline lasers, and particularly fiber lasers, may lead to simpler and inexpensive tunable mid-IR coherent sources [3].

II–VI chalcogenide crystals e.g. ZnS, ZnSe doped with  $\text{Cr}^{2+}$ ,  $\text{Fe}^{2+}$  and  $\text{Co}^{2+}$  have enabled in recent years highly efficient, powerful and versatile laser systems [4] spanning the 1–6  $\mu\text{m}$  spectral range. Some these systems feature high (30 W) CW power, while other produce ultrashort (< 50 fs) pulses intended for various applications. Furthermore, high energy ultrafast waveguide lasers [5] have also been reported. However, to date, a II–VI fiber laser had not been demonstrated.

Silver halide ( $\text{AgCl}_x\text{Br}_{1-x}$ ) crystals offer good transmission in the 0.4–30  $\mu\text{m}$  spectral range with a refractive index  $2.0 < n < 2.2$ ; they feature good mechanical properties and are non-toxic, non-hygroscopic, and have low phonon cutoff frequencies [6]

of  $\sim 100 \text{ cm}^{-1}$ , mitigating multi-phonon losses in the far IR. These can be extruded into optical fibers [7] used in the range 5–15  $\mu\text{m}$ , having a minimum loss of 0.2 dB/m at 10  $\mu\text{m}$ . Studies featuring silver halide crystals doped with rare-earth impurities [8,10] had been carried out in the past, but most of these doped crystals turned out less suitable for practical laser applications. During recent years, we successfully grew and improved the optical quality of transition metal doped crystals. These are found to be promising candidates for a solid-state laser, which could potentially serve as a basis for a mid-IR fiber laser.

Recently, nickel [9], iron [11] and cobalt [12, current work] doped silver halide crystals were grown using the vertical Bridgman–Stockbarger technique. Attempts of doping  $\text{AgClBr}$  with Cr resulted in black, non-active crystals. We studied various compositions of  $\text{AgCl}_x\text{Br}_{1-x}$  ( $0 \leq x \leq 1$ ) having different doping concentrations. The 10 mm diameter crystals were cut to thin disks and mechanically polished. The optical characterization process consisted of measuring the absorption spectrum of each crystal, followed by the emission spectrum under laser excitation of the relevant middle infrared energy band. Furthermore, emission lifetime measurements were performed at different temperatures, leading to the reconstruction of an energy diagram and the measurement of the respective decay rates. The experimental setups have already been described elsewhere [9,11,12].

Within the framework of a single configuration-coordinate model, assuming the strong coupling typical of our ion–ligand configuration, a measurement of the temperature dependence of

Abbreviations: OPO, Optical Parametric Oscillator; ESA, Excited State Absorption; FTIR, Fourier Transform Infrared spectrometer

\* Corresponding author.

E-mail address: [yuvaltsu@post.tau.ac.il](mailto:yuvaltsu@post.tau.ac.il) (Y. Tsur).

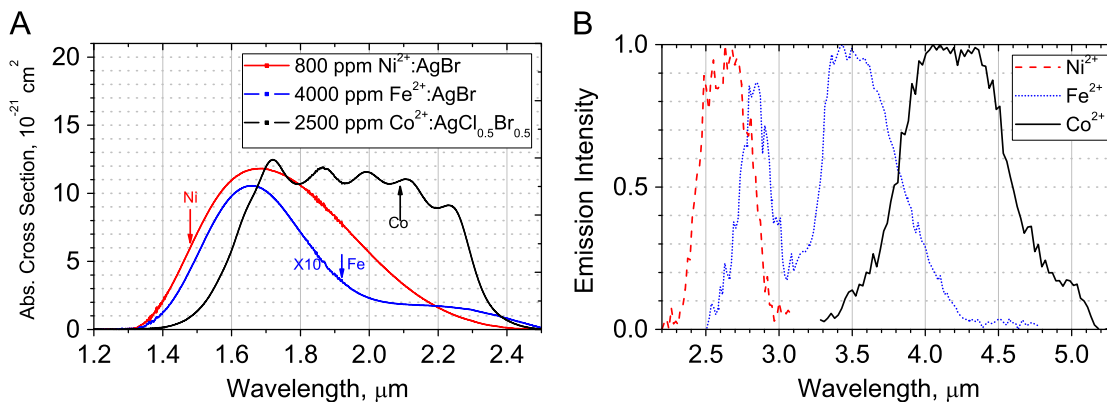


**Fig. 1.** Absorption (A) and emission (B) spectra of silver halides doped with cobalt (black, solid), nickel [9] (red, dashed) and iron [11] (blue, dotted). Ni and Fe show room-temperature absorption and  $T=80$  K emission, while Co shows absorption and emission at  $T=150$  K. The colored arrows in (A) mark the wavelengths of laser excitation for the spectra in (B). The crystalline disc thicknesses were 5.4 mm (Co), 12.0 mm (Ni) and 7.0 mm (Fe), respectively. (For interpretation of the references to color in this figure legend, the reader is referred to the web version of this article.)

**Table 1**

Optical properties of Co, Ni and Fe doped silver halide crystals. Ni and Fe room-temperature absorption and  $T=80$  K emission data are shown, while for Co both absorption and emission data was measured at  $T=150$  K.

Dopant		Co	Ni	Fe	
Host		AgClBr	AgBr	AgBr	
Nominal concentration	$10^{19} \text{ cm}^{-3}$	5.8	1.6	8.0	
Absorption $\lambda$	$\mu\text{m}$	2.1	1.7	1.7	2.1
Absorption cross section	$10^{-21} \text{ cm}^2$	12	12	1.0	0.2
Peak emission $\lambda$	$\mu\text{m}$	4.1	2.7	2.9	3.5
Emission cross section	$10^{-21} \text{ cm}^2$	66	10	–	
Emission lifetime	ms	0.2	2.8	0.085	
Reference		Present work	[9]	[11]	

the emission lifetime allows us to recognize the radiative lifetime  $\tau_{rad}$  as the constant contribution to the rate equation [13]

$$\tau(T) = \tau_{rad}^{-1} + W_a^{-1} \exp\left(-\frac{E_{act}}{k_B T}\right). \quad (1)$$

Here  $\tau(T)$  is the fluorescence lifetime at a temperature  $T$ ,  $W_a$  is associated with the  $T \rightarrow \infty$  non-radiative decay rate,  $E_{act}$  is the energy required for non-radiative activation back to the ground state, and  $k_B$  is Boltzman's constant. Furthermore, emission cross sections were calculated from the emission spectra by using the Futchbauer–Ladensburg relation [15]

$$\sigma_{em}(\lambda) = \frac{1}{8\pi n^2 c \tau_{rad}} \frac{\lambda^5 g(\lambda)}{\int \lambda' g(\lambda') d\lambda'} \quad (2)$$

where  $n$  is the refractive index,  $c$  is the speed of light,  $\tau_{rad}$  is obtained from a best fit to (1) and  $g(\lambda')$  is the emission line shape, normalized to unity at peak emission.

## 2. Results and discussion

The experimental results, describing the near infrared absorption and the mid-IR emission are depicted in Fig. 1(A) and (B) respectively. A summary of the spectroscopic properties appears in Table 1. We note that the nominal concentration column reflects the atomic ratio of the powder constituents. The crystal segments were sawed out of the raw grown crystals according to an a priori spectroscopic criteria of maximum absorption per unit length. Consequently, the selected segments

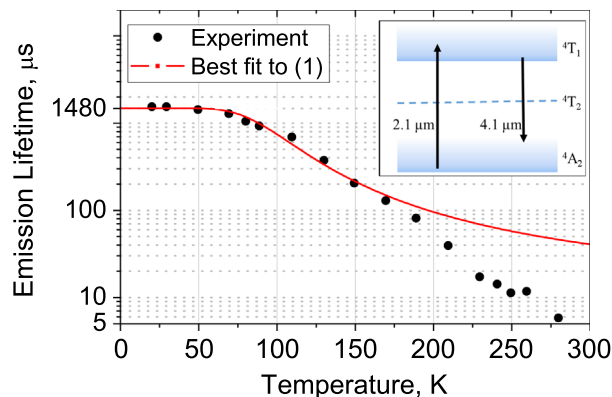


**Fig. 2.** Emission lifetime temperature dependence of the  $5.8 \times 10^{19} \text{ cm}^{-3} \text{ Co}^{2+}:\text{AgCl}_{0.5}\text{Br}_{0.5}$  crystal, along with a best fit to (1). We note that the fluorescence temperature range extends until room temperature, though the lifetime could not accurately be deconvoluted from the detector response. The inset shows the respective schematic energy diagram, where the transition to the  ${}^4T_2$  level is symmetry-forbidden.

necessarily contained a higher dopant concentration than the nominal concentration value.

The spectral analysis shows that cobalt is probably the best silver halide dopant for the development of a solid-state laser, as it features a high emission cross-section and very low relative losses. At high doping levels, a significant portion of the  $\text{Co}^{2+}$  ions are located at interstitial sites having a tetrahedral field symmetry [14], and the absorption spectrum could be interpreted by the energy diagram which appears in the inset of Fig. 2. The transition associated with the Co spectra in Fig. 1 is between the ground  ${}^4A_2$  and the excited  ${}^4T_1$  states, while the transition to the  ${}^4T_2$  level is symmetry-forbidden [14]. This Letter focuses on investigating the feasibility of a cobalt doped silver halide crystalline laser. Firstly, both the radiative and the non-radiative decay rates were measured. The experimental setup utilized an Optical Parametric Oscillator (OPO) made by Opotek (Model Opolette 355II), with the idler beam tuned to  $1.92 \mu\text{m}$ , matching the peak of the absorption band.

The idler beam was directed into a closed-cycle helium cryostat working at the temperature range 20–300 K, coupled with an InSb photodetector (EG&G, Model J10DM204-R07M) having a  $1 \mu\text{s}$  temporal resolution. The detector was fitted with a long pass filter to exclude the excitation signal.

The OPO pulse duration was 9 ns, significantly shorter than the emission lifetime over the whole temperature range. Lifetime measurements at various temperatures were undertaken for the

Download English Version:

<https://daneshyari.com/en/article/5398198>

Download Persian Version:

<https://daneshyari.com/article/5398198>

[Daneshyari.com](https://daneshyari.com)